

## Laser Welding of Stainless Steel Tubes

Hana Chmelíčková,<sup>1</sup> Hana Lapšanská,<sup>2</sup> Helena Hiklová,<sup>3</sup> Martina Havelková<sup>4</sup>

**Abstract:** Laser axial welding is a modern method of production of tubes with seam which are mainly used in automotive and food-processing industry. Welding experiments with AISI 304L stainless steel sheet were conducted using continual high power CO<sub>2</sub> laser with maximal power 5 kW. The aim of these experiments was to evaluate the effect of processing parameters on weld dimensions and surface properties. Subjected parameters were laser power, shielding gas flow and its composition. Modern contact profilometry was applied to display weld surfaces. Metallographic specimens of weld cross sections were prepared to measure the weld area. Temperature field distribution was modeled using finite element software SYSWELD.

**Keywords:** Laser, Welding, Tubes, Process Parameters

### 1. Introduction

Metal tubes are important construction elements in all industry branches. Many production methods have been developed to prepare seamless tubes based on metallurgical semi products. The most commonly used are tube rolling, profiling, extrusion or hydro forming. Various welding methods can be used to prepare seam tubes with required combination of the wall thickness and inside diameter. Beside the tungsten arc welding (GTAW/ TIG) high power laser welding spreads very quickly in tubes production.

Laser tube manufacturing systems usually consist of two main parts, which are few tens meter long tube forming line and a high power laser with a special processing head (Fig. 1) Precise adjustment of forming line rollers is the first necessary condition which has to be fulfilled to prepare quality shape of a tube [1]. The second one is a coincidence of focussed laser beam with weld centreline and required settings of focal plane position with respect to the tube surface. The last but

---

<sup>1</sup> RNDr. Hana Chmelíčková; Joint Laboratory of Optics, Institute of Physics of the Academy of Sciences of the Czech Republic; tř. 17. listopadu 50a, 77207 Olomouc, Czech Republic; hana.chmelickova@upol.cz

<sup>2</sup> Ing. Mgr. Hana Lapšanská; Joint Laboratory of Optics, Institute of Physics of the Academy of Sciences of the Czech Republic; tř. 17. listopadu 50a, 77207 Olomouc, Czech Republic; hana.lapsanska@upol.cz

<sup>3</sup> RNDr. Helena Hiklová; Joint Laboratory of Optics, Institute of Physics of the Academy of Sciences of the Czech Republic; tř. 17. listopadu 50a, 77207 Olomouc, Czech Republic; helena.hiklova@upol.cz

<sup>4</sup> Mgr. Martina Havelková; Joint Laboratory of Optics, Institute of Physics of the Academy of Sciences of the Czech Republic; tř. 17. listopadu 50a, 77207 Olomouc, Czech Republic; martina.havelkova@upol.cz

not least condition is adjusting and keeping the optimal laser processing parameters for each kind of material and its thickness. The effect of chosen processing parameters is studied in this paper.

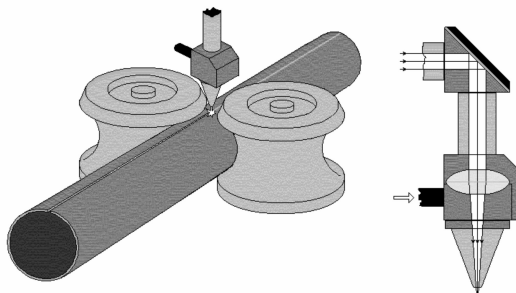


Fig. 1. Scheme of longitudinal tubes welding.

## 2. Experiment

A set of experiments was conducted using laser tube welding system in a private company Vatrans Zlín v.o.s in a production division in Dobrkovice. The aim of these experiments was to study the influence of laser power, pressure and kind of a shielding gas changes on the dimensions and surface characteristics of the weld.

High power continual CO<sub>2</sub> laser ROFIN DC 050 with maximal power 5000 W and wavelength 10.6 μm is implemented into the Profile Welding System (PWS). PWS disposes of a complete beam guiding system with an integrated process sensor system of detection and tracking of the seam gap to ensure safe and reliable laser welding. Processing head has a cooper focussing mirror with focal length 200 mm. Closely Gaussian high quality laser beam with theoretical diameter 0.135 mm comes out from the processing head. In-axis nozzle for processing gas delivery is positioned 10 mm above the weld seam. Processing gas protects focussing mirror against metal spatter. Laser beam focal plane is embedded into the one third of material thickness. Shielding gas is supplied by off axis nozzle.

In our experiments, stainless steel AISI 304 L (Czech equivalent ČSN 17 249) 1 mm thick strip was formed into 63 mm outer diameter tube with 0.003 mm seam gap. Welding speed was set to the optimal value 8 m.min<sup>-1</sup>. This is not a changeable parameter during one process on PWS. When the welding speed is changed the settings of the forming line must be re-adjusted and checked so as the forming speed corresponds to the speed of welding itself. Maximal length of a tube depends on the length of a forming line and used metal strip. Laser cutting machine is implemented to portion welded tube to achieve desired length. In common industrial production, all the welded tubes are usually annealed to reduce internal stresses. We did not do this procedure to study only the effect of process parameters changes without additional treatment.

### 2.1. Variable laser power

Laser power is liable for the heat input into the material which is defined as a portion of laser power and welding speed. Heat input influences weld dimensions and of course penetration depth. The optimal heat input setting is necessary to avoid the lack of penetration. To achieve deep penetration mode in keyhole welding, surface power density must be higher than approximately  $10^6 \text{ W.cm}^{-2}$  [2]. A set of increasing power values in the range from 2780 W to 3750 W was used in the first experiment. All the other parameters were kept constant (Table 1).

**Table 1. Processing parameters with variable laser power**

sample no.	power (W)	in axis gas flow (l.min <sup>-1</sup> )	off axis gas flow (l.min <sup>-1</sup> )	heat input (J.m <sup>-1</sup> )
0	2 780	5	10	20 850
1	3 250	5	10	24 375
2	3 500	5	10	26 250
3	3 750	5	10	28 125

### 2.2. Variable shielding gas flow

Gasses have an important influence on the weld quality. During CO<sub>2</sub> laser welding shielding gas supports the energy input by increasing and stabilisation of laser induced plasma created by ionizing of metal vapours in keyhole, a deep moving capillary following high power welding processes [3]. Argon, nitrogen, helium or a mixture of helium and nitrogen are gasses usually used to protect the weld pool against its oxidation. Shielding gas is delivered by an off axis nozzle. First, argon was used as a shielding gas. Two gas flow values different from the optimal one were tested (Table 2).

**Table 2. Processing parameters with variable shielding gas pressure**

sample no.	power (W)	in axis gas flow (l.min <sup>-1</sup> )	off axis gas flow (l.min <sup>-1</sup> )	heat input (J.m <sup>-1</sup> )
4	3 750	5	17	28 125
5	3 750	5	5	28 125

### 2.3. Variable shielding gas composition

Helium is the best but the most expensive gas for CO<sub>2</sub> laser welding. It has very high ionizing potential and high heat conductivity. Thanks to these characteristics helium ensures the transparency of formed plasma for incident laser beam. Argon can be used to prevent weld pool oxidation. Unfortunately, its ionizing potential is quite low and undesirable additional argon plasma can appear above the weld pool. This plasma absorbs laser beam energy which could lead to poor or other defects. Nitrogen offers excellent plasma suppression but it causes serious spattering and in

combination with certain materials even metallurgical problems like cracks. To join all the advantages of these three gases and suppress their disadvantages including high helium costs, mixtures like helium-nitrogen, helium-argon or helium-oxygen are being used [4].

The last experiment was realized with three different ratios between helium and nitrogen. The other processing parameters were constant and set to their optimal values (Table 3). Gas pressure was adjusted to have its optimal value for helium-nitrogen mixture.

**Table 3. Processing parameters with variable shielding gas pressure**

sample no.	power (W)	in axis gas flow (l.min <sup>-1</sup> )	off axis gas flow (l.min <sup>-1</sup> )	He:N <sub>2</sub>
6	3 750	5	8	50:50
7	3 750	5	8	70:30
8	3 750	5	8	100:0

### 3. Results

Smaller samples 1 cm x 2 cm were cut from each piece of nine welded tubes. Weld surface profile and weld width were measured by the contact profilometer FORM TALYSURF Series 2.

Then, metallurgical samples of weld cross sections were prepared. Polished samples were etched with the mixture of hydrochloric and nitric acid to highlight weld borders and microstructure. Etched weld cross sections were observed and recorded by laser scanning confocal microscope LEXT at magnifications 120 times to 2400 times. Weld dimensions were measured using distance measurement tool of the commercially available software QuickPHOTO Industrial 2.2. The effect of applied process parameters on the weld bead dimensions was evaluated.

Finally, temperature field distribution in cross section was modelled using finite element software SYSWELD.

#### 3.1. Laser power dependence

All the samples were fully penetrated with a typical keyhole cross section shape (Fig. 2). Material microstructure outside the weld is purely austenitic. No conspicuous deformation bands or segregations were observed. This corresponds to the annealed sheet. Weld metal shows typical casting macrostructure. Solidification structure is represented by columnar crystals oriented in the direction of the most intensive heat removal from the melted material to the surrounding metal. Austenitic grain size was approximately the same in weld closest neighbourhood as in the basic material. Grains did not become coarser and no detectable heat affected zone was found using optical microscopy which is typical for laser welding. Deformed austenitic grains practically reached the border of the weld (Fig. 3).

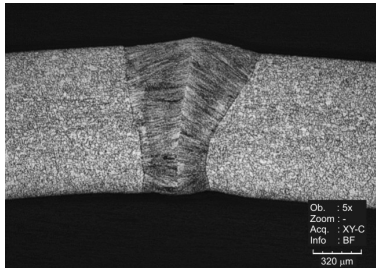


**Fig. 2.** Cross section of the sample no. 1 (magnification 120 times).

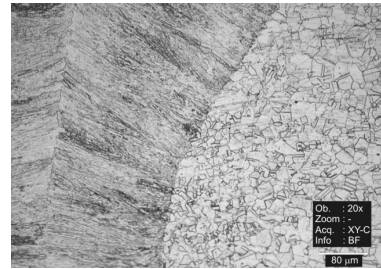


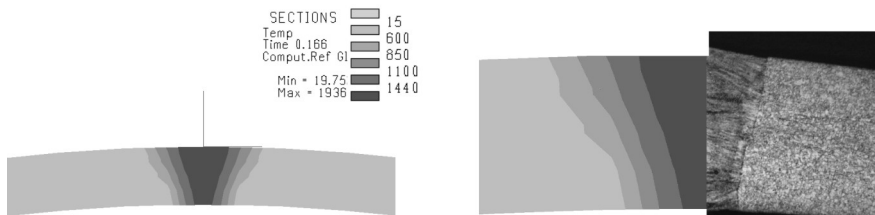
**Fig. 3.** Weld metal - basic material boundary in sample no. 1 (magnification 480 times).

Weld dimensions increase with increasing heat input (Table 4). Bead top width is approximately two times higher in comparison with the bottom width and increases with power from 0.855 mm to 0.962 mm.

**Table 4. Weld dimensions – power dependence**

sample no.	top weld width (mm)	bottom weld width (mm)	weld height (mm)	weld cross section area (mm <sup>2</sup> )
0	0.855	0.298	1.066	0.555604
1	0.916	0.451	1.049	0.603477
2	0.928	0.449	1.054	0.640506
3	0.962	0.472	1.083	0.656027

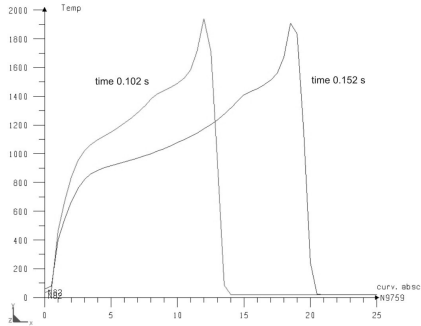
Temperature field distribution in weld cross section and its comparison with the real cross section of sample no. 1 presents Fig. 4. Maximal achieved weld pool temperature was 1936 °C.



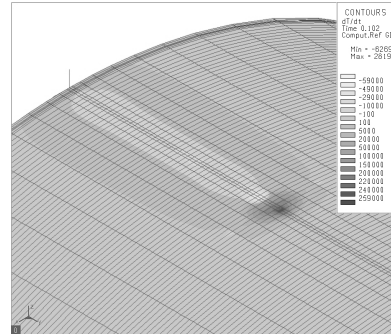
**Fig. 4.** Temperature field distribution in laser affected zone (sample no. 1).

Figure 5 shows temperature-distance dependence for two different time moments. Time difference between these two moments is 0.05 s which corresponds to the distance 6.7 mm on the weld seam. Curve peak matches laser source position along the welding trajectory. Step temperature decrease after reaching the maximum represents a very high heating rate. Beam affected area is very narrow. Only about 2 mm ahead of a source position are affected at given time. Maximal

heating rate at the node was almost  $3 \cdot 10^5 \text{ }^\circ\text{C} \cdot \text{s}^{-1}$  (positive values in Fig. 6). On the other hand cooling rates (negative values) are much lower in their absolute values.



**Fig. 5.** Temperature-distance dependence for two different time moments.



**Fig. 6.** Temperature rate distribution at 0.102 s.

### 3.2. Shielding gas flow dependence

Weld material surface depression along the right side of the weld line was observed on at each sample. This is caused by off axial flow of a shielding gas. Cross section profiles were selected from data captured by contact profilometer. Fig. 7 and Fig. 8 show weld profiles with evident difference in vertical properties. The higher shielding gas flow the more distinctive vertical differences. Optimal gas flow must be found in each application.

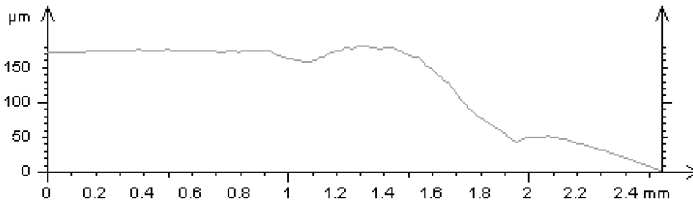


**Fig. 7.** Surface profile of the sample no.5, gas flow  $5 \text{ l} \cdot \text{min}^{-1}$ .

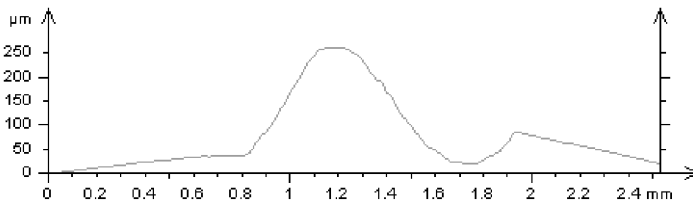


**Fig. 8.** Surface profile of the sample no.4, gas flow  $17 \text{ l} \cdot \text{min}^{-1}$ .

### 3.3. Mixture composition dependence

Continual 3D reconstructions show significant differences between weld bead surfaces (Fig. 9 and Fig. 10). Profile smoothness arises with increasing amount of helium in the shielding gas mixture. A reasonable compromise between quality and economy aspects must be found in industrial production.

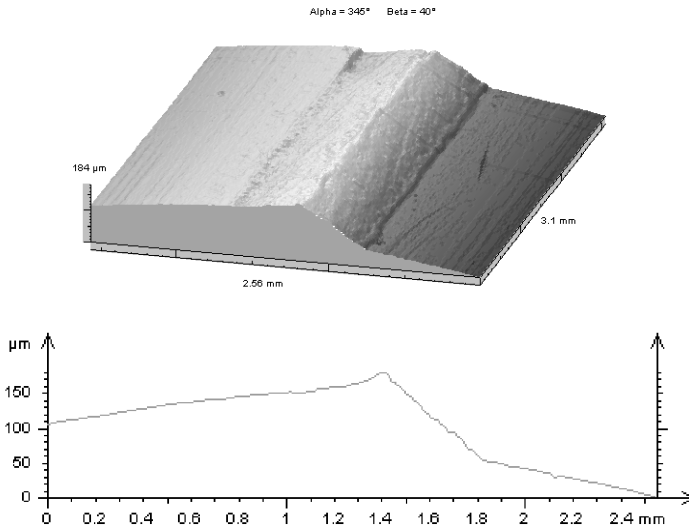


Fig. 9. 3D surface reconstruction and selected profile of the sample no.6.

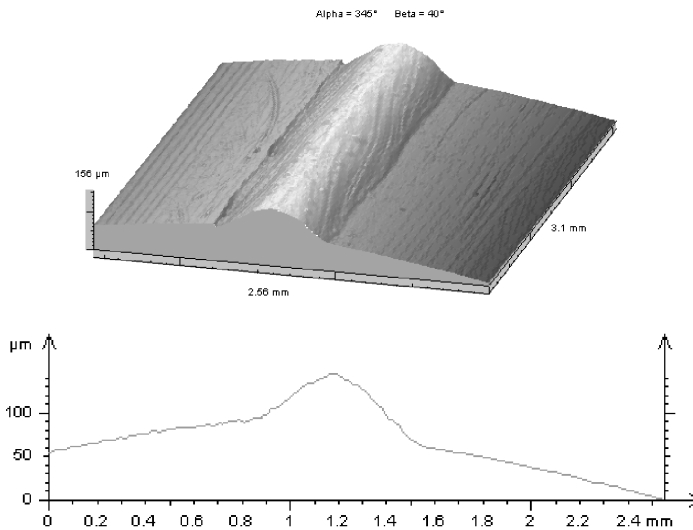


Fig. 10. 3D surface reconstruction and selected profile of the sample no.8.

#### 4. Conclusions

A set of experiments with variable laser processing parameters was realised using Profile Welding System with the tube forming line in a company Vatrans Zlín v.o.s. Laser power, shielding gas flow and mixture gas composition were modified to values different from the optimal. Result weld bead dimensions, surface characteristics and temperature field distribution in the heat affected zone were evaluated by means of the contact profilometry, laser confocal microscopy and metallographic analyze.

#### Acknowledgements

The Academy of Sciences of the Czech Republic supports this work under the project no. KAN301370701.

#### References

- [1] "ROFIN DC Series," Technical data, *Available from* [http://www.rofin.com/en/products/cosub2sub\\_lasers/slab\\_laser/dc\\_series/](http://www.rofin.com/en/products/cosub2sub_lasers/slab_laser/dc_series/)  
*Accessed:* 2010-04-13.
- [2] Ion J.C., *Laser Processing of Engineering Materials* (Elsevier, Oxford, 2005). ISBN 0-7506-6079-1.
- [3] Dowden J., "Laser Keyhole Welding: The Vapour Phase," in *The Theory of Laser Material Processing*, Dowden J., ed., (Springer Science+Business media B.V., Dordrecht, 2009), pp. 97-98. ISBN 13-978-1-4020-9339-5.
- [4] Wirth P., *Introduction of laser material processing* (ROFIN, Hamburg, 2009), pp. 12-22.